RSC Advances

Synthesis, Characterization of Quantum Dots and their Application as Laser Soft Desorption/Ionization for Labile Metal-Drug Interactions and their Antibacterial Activity

Journal:	*RSC Advances*
Manuscript ID:	RA-COM-06-2015-011301.R2
Article Type:	Paper
Date Submitted by the Author:	07-Aug-2015
Complete List of Authors:	Abdelhamid, Hani; NSYSU, chemistry department Wu, Hui Fen; National Sun Yat-Sen University,

Synthesis, Characterization of Quantum Dots and their Application as Laser Soft Desorption/Ionization for Labile Metal-Drug Interactions and their Antibacterial Activity

Hani Nasser Abdelhamid[1,2], Hui-Fen Wu[1,3,4,5]*
[1]Department of Chemistry, National Sun Yat-Sen University, Kaohsiung, 804, Taiwan
[2]Department of Chemistry, Assuit University, Assuit, 71515, Egypt
[3]Center for Nanoscience and Nanotechnology, National Sun Yat-Sen University, Kaohsiung, 804, Taiwan
[4]Doctoral Degree Program in Marine Biotechnology, National Sun Yat-Sen University, Kaohsiung, 804, Taiwan
[5]School of Pharmacy, College of Pharmacy, Kaohsiung Medical University, Kaohsiung, 800, Taiwan
* Corresponding author. Phone: 886-7-5252000-3955. Fax: 886-7-525-3908.
E-mail: hwu@faculty.nsysu.edu.tw
Contract/grant sponsor: National Science Council (NSC), Taiwan

Abstract

Synthesis, characterization of quantum dots modified mercaptopropionic (CdS@MPA) and their application as laser soft desorption/ionization for labile metals-drugs interaction was reported. CdS@MPA was synthesis via hydrothermal and characterized using TEM, UV-vis absorption, fluorescence, and FTIR spectroscopy. These tiny nanocrystal (< 5 nm) provide large surface area and UV-vis absorption that in good matches with N_2 laser (337 nm) of matrix assisted laser desorption/ionization mass spectrometry (MALDI-MS). Thus, it softly desorbs/ionize labile metallodrug without destroy of the weak noncovalent bonds between the drug and the heavy transition metals (HTMs). Because the UV absorption at 337 nm and large surface area, the present technique has coined as quantum enhanced laser desorption/ionization mass spectrometry (QELDI-MS). Detection of the interaction of HTMs and non-steroidal anti-inflammatory drugs (NSAIDs) in aqueous solution is critical because these coordination are weak and labile for acid solution of conventional matrices. QELDI-MS presented high performance and low limit of detection (0.5 μL, 0.1-0.5mM) for metallodrug detection in

aqueous solution. The antibacterial activities of the metallodrugs against pathogenic bacteria were investigated using optical density (OD_{600}), cell counting and proteomics analysis. Simple detection of the metallodrug in aqueous solution is promising for environmental, biological and analytical concerns.

Keywords: Metallodrug, soft ionization, mefenamic acid, surface enhanced laser desorption/ionization mass spectrometry (QELDI-MS), pathogenic bacteria, quantum dots.

Introduction

Semiconductor nanocrystals or quantum dots (QDs) have been received numerous attentions for many and diverse trends [1-7]. They could serve for many applications such as photocatalysis, light emitting diodes (LEDs), sensing labeling….etc[1-11]. Nanocrystals, with size less than 10 nm, offer distinctive features such as large surface area, unique photo-properties that are absent in bulk material, have small energy gap, offer long life-time, flexible for structure modification via surface changes or doping, and abundantly produce in large scale [1-9]. They also could serve as surface assisted laser desorption/ionization laser ionization mass spectrometry (SALDI-MS) [12-17].

The coordination of drugs to biological metal ions could improve the pharmaceutical efficacy and increase the interaction with the cells biomolecules such as protein, DNA …etc due to the unique characteristics of metal complexes. It could provide a store for new and effective drug under a broad name called metallodrug. Thus, general and large interests were invested for the study of the influential effect of these species on the human health and for environmental concerns. These metallodrugs could interact with protein bovine pancreatic ribonuclease (using Auoxo6) [18], human serum albumin (HSA, for platinum (IV) prodrugs) [19], DNA (for polypyridyl

copper (II) complexes) [20], or other biomolecules species [21]. Non-steroidal anti-inflammatory drugs (NSAIDs) are wide spread drugs that provide analgesic, antipyretic, and anti-inflammatory effects [22]. The interactions of heavy transition metals (HTMs) such as abundant biological metals (Cu^{2+}, Fe^{2+}, Fe^{3+}, …etc) are critical for human being. However, these interactions are labile for the harsh condition of various analytical tools [23-24]. Thus, a new and effective analytical methodology is highly required for detection of these species in aqueous solution. Furthermore, the structures of many metal-NSAID complexes are not well characterized [25].

Mass spectrometry (MS) has been intensively used for drugs, biomolecules or metallomics [24]. Electrospray ionization mass spectrometry (ESI-MS) and matrix assisted laser desorption/ionization mass spectrometries (MALDI-MS) are soft ionization techniques [26-27]. However, the latter i.e MALDI-MS faces many challenges as the conventional organic matrices are often organic acids such as 2,5-dihydroxybenzoic acid (DHB), α-cyano-4-hydroxycinnamic acid (CHCA), mefenamic acid, furoic acid …etc. These acids destroy the non-covalent interactions between the metal and drug moieties [22]. Furthermore, it could form cluster with the metal centers, produce interference signals and form adduct ions with the metal complexes [28-29]. Thus, improvement and advances in metallodrug analysis using MALDI-MS enable a rational and more tailored drug design because the technique could screen the metallodrug-protein interaction directly and provide the screening for cellular- drug interactions [30].

Herein, we presented fast, soft, and direct detection of the interaction among non-steroidal anti-inflammatory drug (NSAIDs) and heavy transition metals (HTMs) such as “Cu(II), and Fe(III)” using CdS quantum dots (CdS@MPA) enhanced laser desorption/ionization mass

spectrometry (QELDI-MS). Mefenamic acid was selected as NSAIDs model because their well-known toxicity such as hepatotoxicity, nephrotoxicity and gastrointestinal toxicity [31]. CdS modified mercaptopropanoic acid (CdS@MPA) was synthesized and characterized using TEM, UV-vis absorption, fluorescence and FTIR. CdS@MPA offered absorption at 337 nm that matches with the wavelength of N_2 laser (λ= 337 nm) of MALDI-MS. Thus, it serve as quantum enhanced laser desorption/ionization mass spectrometry (QELDI-MS). The detection requires tiny volume (2 μL) and reported no destroy of the weak coordination between the metal centers and the drug. The cytotoxicity of the metallo-drug against two pathogenic bacteria (*Pseudomonas aeruginosa* (*P. aeruginosa*) and *Staphylococcus aureus* (*S. aureus*)) was investigated using MALDI-MS, cell counting and optical density (OD_{600}).

Chemicals

$CuSO_4.5H_2O$ and ponstel drug (was used as pure mefenamic acid without any additives) were purchased from Sigma Company (China). Mercaptopropanoic acid (MPA) and cadmium nitrate (99.0%) were purchased from Sigma–Aldrich (Australia). 2,5-dihydroxybenzoic acid (DHB) and $FeCl_3.6H_2O$ were purchased from Riedel-de Haën (Seelze, Germany). Sinapinic acid was purchased from Alfa Aëser (Great Britain). Methanol (HPLC grade) was purchased from Merck (USA). All the chemicals were used directly without further purification. De-ionized water (18 MΩ purified Millipore water, USA) was used for preparation all solutions.

Instruments

pH and conductivity measurement

pH and conductivity (S cm^{-1}) of the drug and the metallodrug solutions were measured by Istek pH meter (Seoul, Korea). All structures and mass calculations were measured by software program ACD-Chemsketch V12.

MALDI-TOF Instrument

The MALDI-TOF-MS analyses were performed by employing positive ion mode on a time-of-flight mass spectrometer (Microflex, Daltonics Bruker, Bremen) with a flight tube, nitrogen laser, pulse width and accelerating potential were 1.25 m, 337 nm, 3 ns, +20 kV, respectively. The spectra were obtained by the averages of 100-200 laser shots. The laser power was adjusted slightly above the threshold to obtain good resolution and high signal-to-noise (S/N) ratios. The complexes were recorded in the reflectron mode, while the bacteria were detected in the linear ion mode using positive mode.

Experimental Section

Preparation of Quantum dots (CdS@MPA)

CdS@MPA quantum dots were prepared from cadmium nitrate and sodium sulphide by capping with mercaptopropanoic acid (MPA). Typically, 400 µL of 3-MPA was mixed in 15 mL deionised water deoxygenized with fresh N_2 gas and then stirred for 1 h after mixed with 2 mL of cadmium nitrate solution (10 mM) was added under N_2 gas and stirring for 1 h. pH of the solution was adjusted to 9 by adding ammonium hydroxide solution. Then, a fresh solution of sodium sulphide (2.5 mL, 8 mM) was quickly added to the above solution at 96 °C and was stirred for 2 h to get green yellowish CdS@MPA. The material was stored in refrigerator before the use.

pH and conductivity measurements

10 mL of ponstel drug (1 mM) was mixed with 5 mL of each metals solution (1mM) and incubated 10 min before measurements. All measurements were recorded at 25 ± 2 °C.

MALDI-MS and QELDI-MS measurements

About 10 μL of ponstel drug (1mM) was mixed with the appropriate molar ratio of metal solutions (10 μL, 1mM) based on molar ratio with 10 μL of conventional matrix 2,5-DHB (50 mM) or quantum dots (CdS@MPA). Then, about 2 μL of the mixed solution was spotted in MALDI plate and kept for drying before use.

Bacteria Cultivation

Both bacteria *Staphylococcus aureus* (BCRC 10451) and *Pseudomonas aeruginosa* (BCRC 10303) were cultivated using conventional method. *S. aureus* and *P. aeruginosa* standard cultures were purchased from Bioresource Collection and Research Center (Hsin-Chu, Taiwan). The bacterial cultures were stored in powdered solid-phase (lyophilized) and were recovered by aseptically adding 0.3-0.5 mL of appropriate liquid medium. Then, 0.1-0.2 mL of the re-suspended culture was streaked directly onto an appropriate agar plate and incubated at 37 °C. The bacteria were cultured repeatedly into fresh medium every two days for a week (sub-culturing) before using.

Biological Assay

Bacteria (500 μL) was incubated with 10 μL (1mM) of amoxicillin (as reference), ponstel drug, and the complexes (Fe(III) and Cu(II)), individually. Bacteria were counted after 3h and 24 h by the plate counted and optical density at wavelength 600 nm (OD_{600}).

Results and Discussion

Characterizations of CdS QDs capped with MPA (CdS@MPA)

Quantum dots (CdS) modified MPA (CdS@MPA) were synthesized via solvothermal method and characterized using transmission electron microscopy (TEM), Fourier transform infrared (FTIR), UV-vis absorption and fluorescence spectroscopy as shown in Figure. 1 (A-D). TEM image (Figure. 1A) reveals that the predominant size is about 1-5 nm with average size 1.28 nm. The distribution histogram of the CdS@MPA particles is plotted in the inset of Figure 1A. CdS@MPA QDs display absorption at 300-450 nm (Figure. 1B) that can be proved from the green-yellowish color as shown in the inset of Figure.1B. According to the empirical equation 1 [32], the average size of CdS@MPA quantum dots is 1.34 nm, which completely agree with the average size of TEM (Figure. 1A). The excitation wavelength at λ_{ex} = 295 nm offers fluorescence emission peak at 595 nm corresponding to transition of electrons from shallow states near the conduction band to sulfur vacancies present near the valence band (λ_{ex}= 295 nm) as shown in Figure 1C. Capping of CdS QDs with MPA (CdS@MPA) is confirmed via FTIR (Figure.1D) that show peaks at wavenumber 3400, 1715 and 1100 cm^{-1} which are assigned as O—H, C=O, and C—O, respectively. The weak peaks due to C—H stretching are observed at about 618 cm^{-1}. It was observed that the sulfuryl band (—SH) at 2570 cm^{-1} are absent that indicated MPA had been successfully capped onto the surface of CdS QDs and form Cd—S.

$$\mathbf{D = (-6.6521 \times 10^{-8})\lambda^3 + (1.9557 \times 10^{-4})\lambda^2 - (9.2352 \times 10^{-2})\lambda + (13.29)} \quad \text{……..Eq.1}$$

Where, D (nm) is the size of a given nanocrystal sample, and λ (nm) is the wavelength of the first excitonic absorption (Figure 1B).

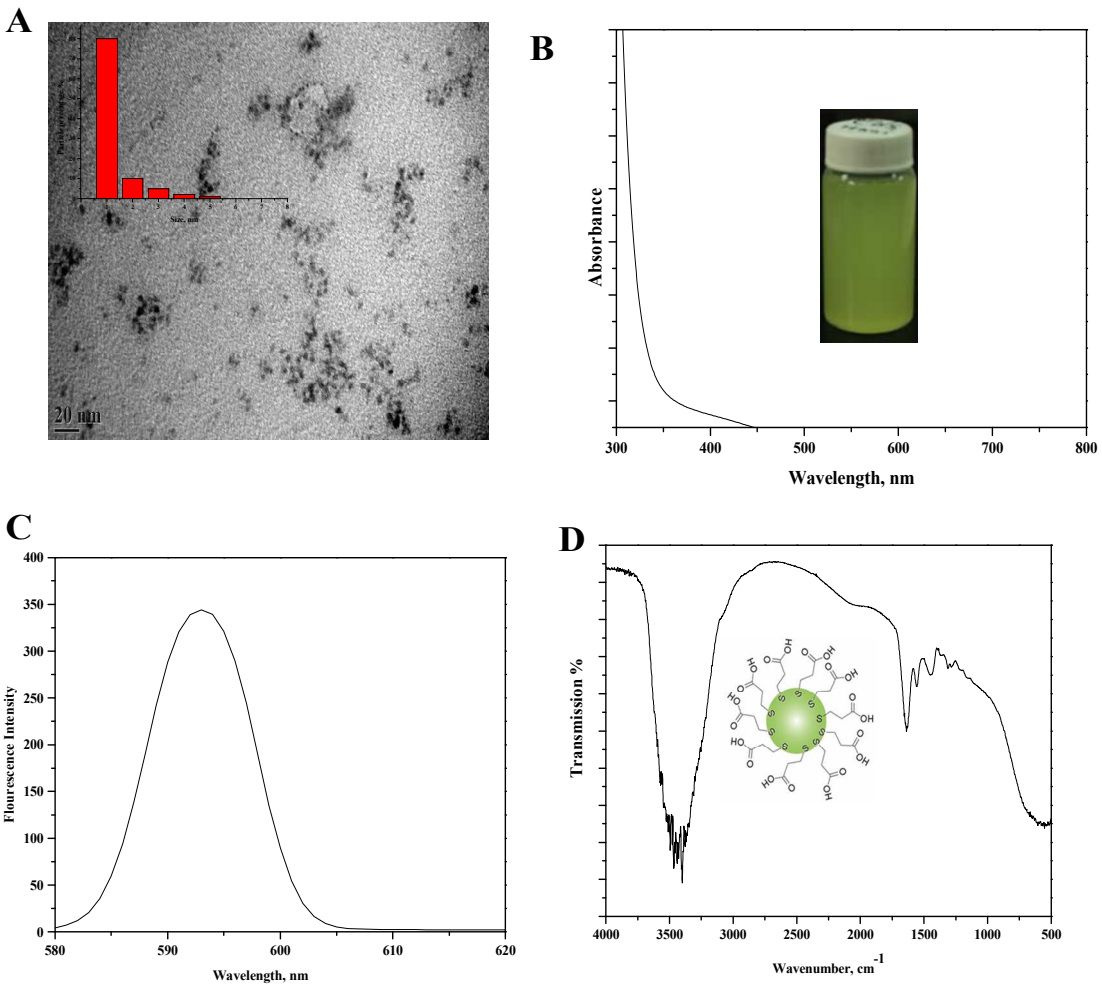

Figure 1: Characterization of synthesized CdS@MPA using (A) TEM, (B) UV-vis absorption, (C) fluorescence spectroscopy and (D) FTIR spectroscopy

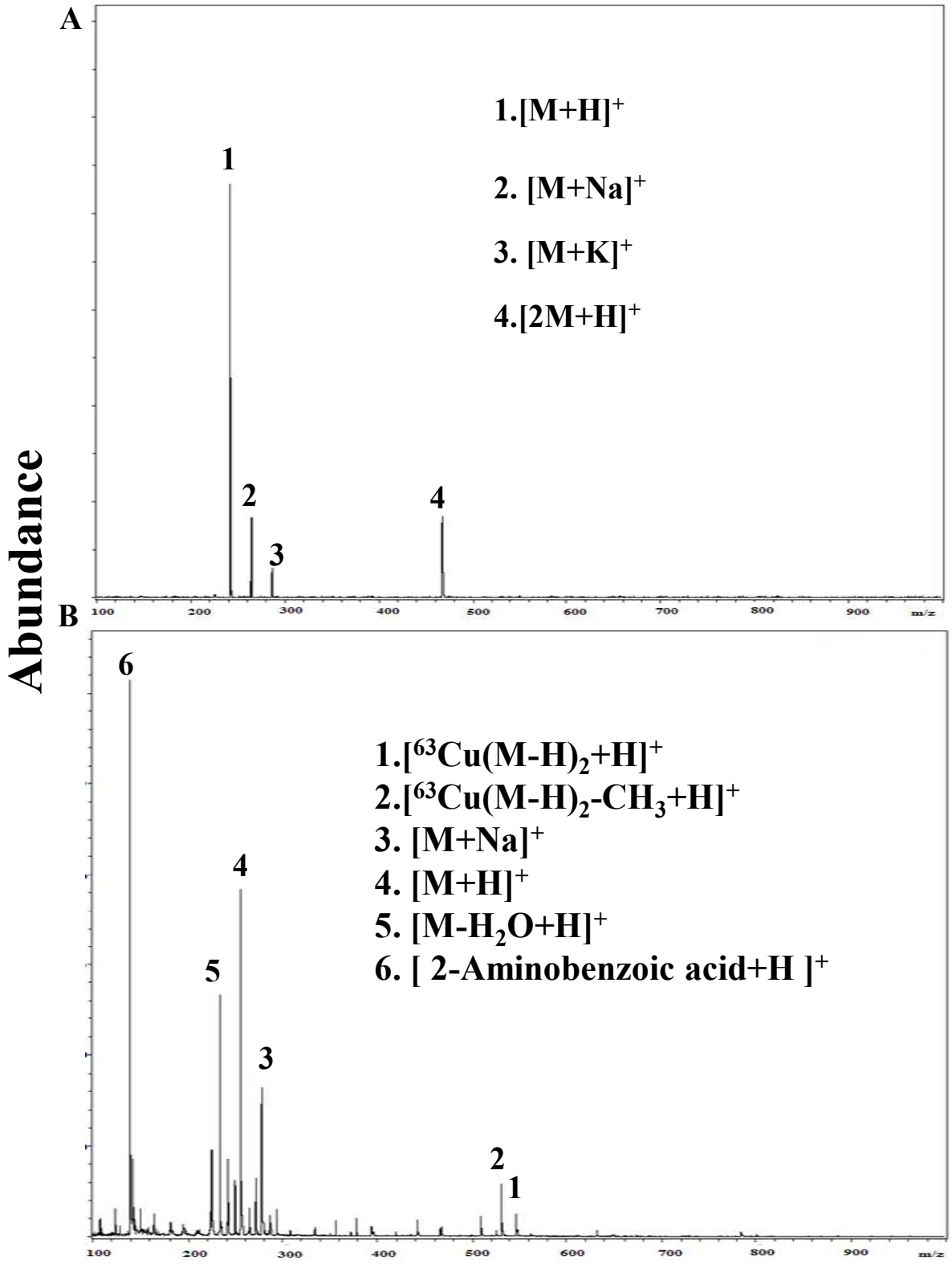

Figure 2: QELDI-MS spectra of (A) ponstel drug and (B) Cu-ponstel complex.

Quantum enhanced laser desorption/ionization (QELDI)–MS of ponstel drug

Non-steroidal anti-inflammatory drug named ponstel drug (M), has a nominal mass 241.2 Da. Quantum dots enhanced laser desorption/ionization mass spectrometry (QELDI-MS) (Figure 2A) display peaks at *m/z* 242.1 corresponding to the protonated drug i.e $[M+H]^+$. The peak at *m/z* 265.2 and 281.2 are corresponding to the $[M+Na]^+$ and $[M+K]^+$, respectively. QELDI-MS didn't disturb non-covalent bond in dimer peak (*m/z* 465, $[2M-H_2O+H]^+$), thus it is a soft ionization over than traditional MALDI-MS technique (Figure S1).The peaks assignments are tabulate in Table S1. QELDI-MS (Figure 2A) shows high resolution. Due to the soft ionization of QDs (CdS@MPA) using QELDI-MS technique, it is proposed as surface to probe the non-covalent bond for metallodrug analysis. The good matches of UV absorption of CdS@MPA with the wavelength of N_2 laser enhance the desorption/ionization process.

pH, conductivity and spectroscopic techniques

Ponstel drug is N-anthranilic acid derivatives that have carboxylic and amine groups as main function groups. To probe the binding sites of the drug, pH and conductivity are measured and are tabulated (Table 1) as preliminary and quick tools. Data showed drop in pH and increase of conductivity may be due to liberation of H^+. UV-vis absorption of Cu(II)-ponstel (Figure 3A) and Fe(III)-ponstel (Figure 3B) probe the metallodrug formation in liquid phase. UV-vis spectra (Figure 3(A-B)) of ponstel drug displays absorption at 337 nm which coincide with the wavelength of nitrogen laser (337 nm), so laser desorption/ionization-mass spectrometry (LDI-MS) shows drug peak at 241.1 Da (Figure. S1A)[33]. Absence of the UV-vis absorption at 337 nm of the two metallodrugs (Figure 3(A-B)) makes the metallodrugs undetectable using LDI-MS (Figure S1(B-C)). Conventional matrix (2,5-DHB) offers a lot of interference as shown in Figure. S2A that disturbs the non-covalent interactions in metallodrug (Figure S2(B-C)) and

generates clusters with metallodrug complexes that complicates the mass spectra. Thus, we apply CdS@MPA quantum dots that show low interference, soft ionization and do not disturb the noncovalent interactions among the metals and drug.

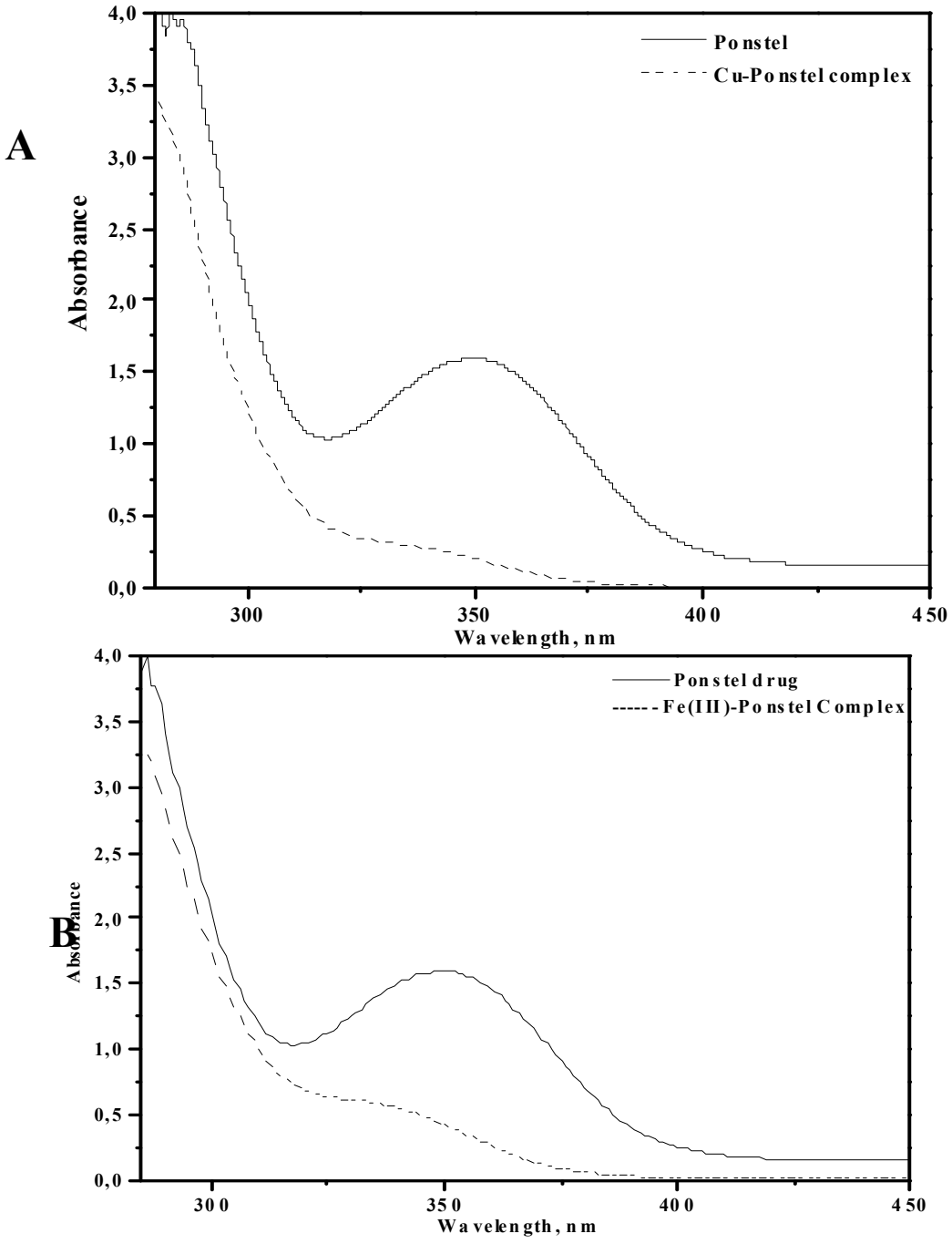

Figure 3: UV-vis absorption of the drug and its complexes for (A) Cu (II)-ponstel and (B) Fe(III)-ponstel complex.

Transition metal complexes of the drug

It was reported that ponstel drug can react with the different metals at ambient temperature, physiological pH (i.e 7.4) and contact time 10 min [34]. QELDI-MS of metal complexes were reported in Figure. 2b and Figure. S3 for Cu(II) and Fe(III), respectively. QELDI-MS shows peak at *m/z* 543.0 Da that assigned as $[^{63}Cu(M\text{-}H)_2+H]^+$ (Figure . 4B). The peaks belong to the drug (<300 Da) are assigned as mention previously (Table S1). The base peak (most abundant peak) at *m/z* 137.0 Da corresponding to [2-aminobenzoic acid+H]$^+$. QELDI-MS of the Fe(III)-ponstel complex was shown in Figure. S3. Spectra show peak at *m/z* 777.0 Da that can assigned as $[^{56}Fe(M\text{-}H)_3+H]^+$. Peak assignments are tabulate in Table S1 and limit of detection in Table 2. The main advantages of QELDI-MS are that a small volume of samples is sufficient for analysis; usually 0.5 μL (5mM) can be analyzed. QELDI-MS is highly tolerated to high inorganic salts concentration, so that it is suitable for analysis the metallodrug in biological.

Biological assay against pathogenic bacteria

For real measurement of the influential effect of metallodrug on the biological cells, pathogenic bacteria were used. Formation of metallodrug in aqueous solution could cause cytotoxicity because the direct imbalance of the eco-system. First, the free metal such as Cu(II) or Fe(III) changes to metal complex forms. These metal centers in the new species have dramatic and different properties over the free metals. Second, the function groups of the free drug change and the main reactive groups have been omitted. Third, the new species have dramatically different chemical and physical character over the two main components. Thus, evaluation of the cytotoxicity/biocompatibility is highly required.

Pseudomonas aeruginosa is Gram-positive. It is pathogenic bacterium that causes inflammation, while *Staphylococcus aureus* is Gram-negative bacteria. To understand the biological activity of the drug and its complexes against the bacteria, amoxicillin are used as a reference that shows inhibition to both bacteria. MALDI-MS reveals a direct evaluation of the drug/metallodrug interactions against *P. aeruginosa* (Figure. 4A) and *S. aureus* (Figure. 4B) after short time (3h) and long time (Figure. S4-S5). MALDI-MS provide a useful tool for the cytotoxicity evaluation as pathogenic bacteria adapt very rapidly with the environmental [35-38]. Because the complexity of the bacteria cell, a standard experiment was carried as a control experiment. The comparison between the bacteria after and before the interaction was evaluated. This is a comparative measurement, especially MALDI-MS data depend on several factors such as bacteria cultivation time, sample treatment, matrix, …etc.. Quantum dots (CdS@MPA) has been avoided because their intrinsic cytotoxicity against the pathogenic bacteria [39]. These interactions are known to exert a great impact on the mode of action of these compounds, including drug metabolism, delivery, cell processing, and targeting. MALDI-MS data reveals high binding of the drug over than their metallodrug. It was reported that mefenamic acid and diclofenac inhibited all uridine 5′-diphospho-glucuronosyltransferase (UGT) enzymes (i.e. UGT1A1, 1A3, 1A4, 1A6, 1A9 and 2B7) in human liver microsomes (HLMs) UGTs tested [40]. The mechanistic study of mefenamic acid activity is mainly due to induction of L-selectin shedding [41].

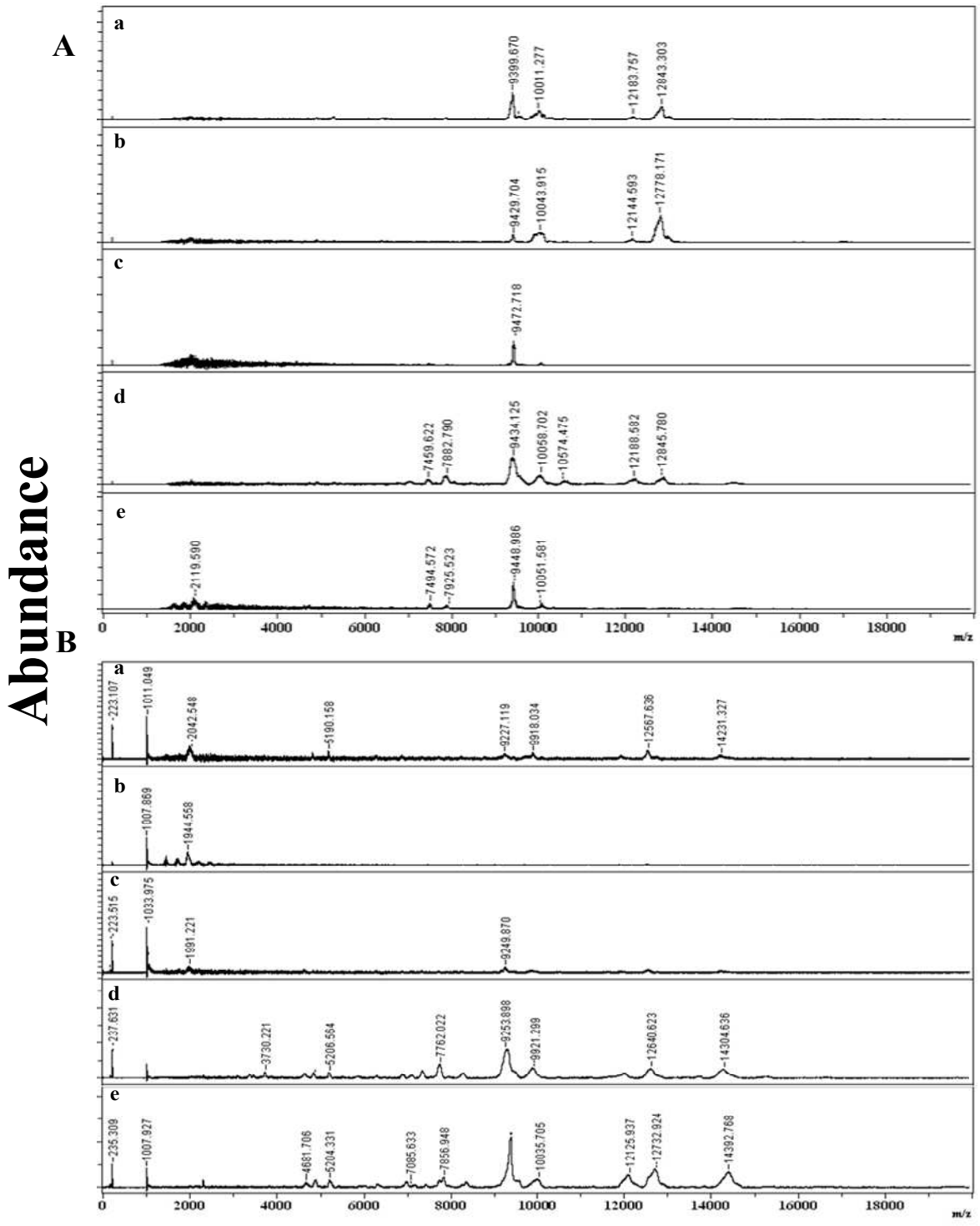

Figure 4: MALDI-MS spectra of biological assay after 3h incubation for (A) *Pseudomonas aeruginosa,* and (B) *Staphylococcus aureus* before (a) and after interaction with (b) Ponstel drug acid, (c) amoxicillin, (d) Cu(II)- Ponstel drug complex and (e) Fe(III)- Ponstel drug complex

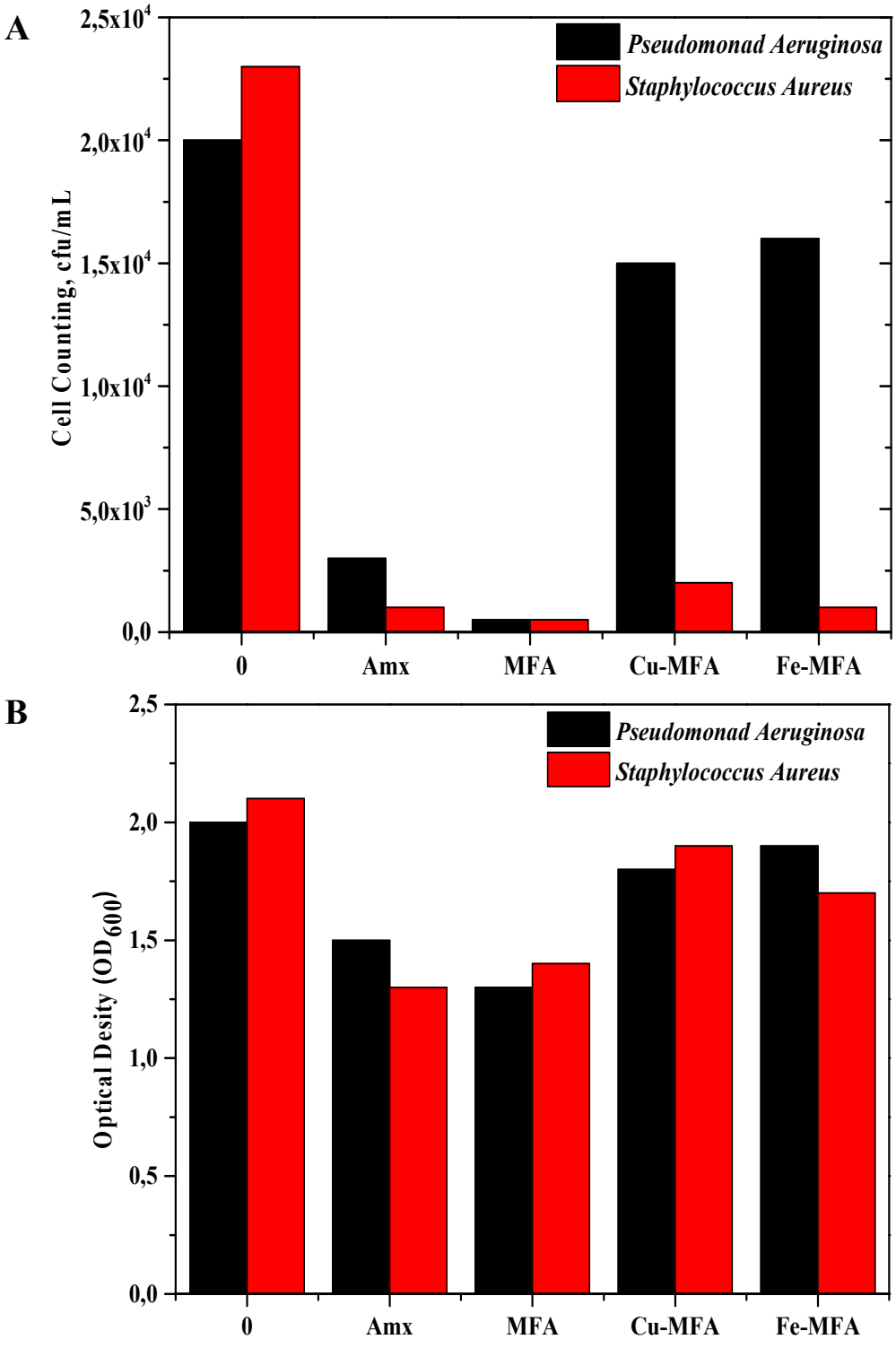

Figure 5. Biological Assay using (A) cell counting and (B) Optical density (OD_{600})

To confirm and support the MALDI-MS data, plate counting (Figure. 5A) and optical density data (OD_{600}, Figure. 5B) were investigated. Data reveals biocompatibility or low cytotoxicity of the two metallo-drug comparing to the parent drug. Cytotoxicity of the latter is due to high binding affinity toward proteins or DNA. Copper(II) complexes with mefenamic acid in the presence of aqua or nitrogen donor heterocyclic ligands (2,2′-bipyridine, 1,10-phenanthroline, 2,2′-bipyridylamine or pyridine) showed interaction of the complexes with calf-thymus DNA (CT DNA) [42]. While, metallodrug offer low protein bound due to increase hydrophilicity and shielding carboxylic group. It was reported that mefenamic acid significantly depressed plasma thyroxine (T4) and thyroidectomized, T4-maintained rats within 3 h in man [43]. The pharmaceutical effects of three manganese-mefenamic acid (Mn-mef) complexes were investigated and data exhibited higher lipoxygenase (LOX-1) inhibitory activity than the parent ligand mefenamic acid [44]. This higher efficiency are due to presence of Mg metal centers. Co(II)-mefenamic acid complexes ($[Co(mef)_2(MeOH)_4]$, or $[Co(mef)_2(MeOH)_2(N\hat{}N)]$ (where mef = mefenamic acid and N^N = 2,2′-bipyridine, 1,10-phenanthroline or $(pyridine)_2$) showed stronger free radical scavenging abilities of the complexes against 2,2-diphenylpicrylhydrazyl (DPPH) free radical scavenging activity than mefenamic acid [45]. The activities of Ni-based complexes were also reported [46]. They showed binding to serum albumin [46]. The binding of the metallodrug to the protein make the detection of the metallodrug in presence of the pathogenic bacteria is difficult task. It is important to stress that the cytotoxicity of the metallodrug against the bacteria was evaluated after incubation for long time (3-12 h). The incubation could change the structure of the metallodrug. Furthermore, metallodrug could bind to the cell biomolecules such as carbohydrate, lipopolysaccharides (LPS), proteins, DNA, ..etc [43-46]. Thus, it is difficult to detect these species in presence of the bacteria cell molecules. These questions require several

steps such as separation of the binding biomolecules followed by crystallization in order to prove the binding affinity using X-ray diffraction or other techniques. We try to answer this question using mass spectrometry in the near future. In summary, mefenamic acid is rich ligand for metal, even precious metal such as Pd [47]. Thus, they serve for many applications such as antibacterial agents (as reported here), catalysis, energy …etc.

Conclusion

Quantum dots (CdS) offer a promising ability to detect metallodrugs (*m/z* <1000Da) without disturbance of the weak non-covalent interaction. Furthermore, QELDI-MS provided free interference with remarkable low limit of detection. QELDI-MS is high resolution, low sample load and soft ionization for the metallodrug detection. Biological assay discern low cytotoxicity of metallodrug versus the parent drug. QELDI-MS may be has a potential application to detect/analysis metallodrug in biological samples. It could be used as a new tool to monitor the drug and their metallodrugs in aqueous solution.

References:

1. L. W. Wang, *Science*, 2014, **344**, 1380–1384; (b) M. P. Moloney, J. Govan, A. Loudon, M. Mukhina and Y. K. Gunko, *Nat. Protoc*., 2015, **5**, 558–573.
2. G. Zhu, K. Yang and C. Y. Zhang, *Chem. Commun*, 2015, 51, 6808–6811.
3. J. L. Wang, G. H. Chen, H. Jiang, Z. Y. Li and X. M. Wang, *Analyst*, 2013, **138**, 4427–4435.
4. J. B. Blanco-Canosa, M. Wu, K. Susumu, E. Petryayeva, T. L. Jennings, P. E. Dawson, W. R. Algar and I. L. Medintz, *Coord. Chem. Rev*. 2014, **263**, 101–137.
5. X. Dai, Z. Zhang, Y. Jin, Y. Niu, H. Cao, X. Liang, L. Chen, J. Wang, X. Peng. *Nature*, 2014, **515**, 96–99.

6. Y. Yang, Y. Zheng, W. Cao, A. Titov, J. Hyvonen, J. R. Manders, J. Xue, P. H. Holloway , L. Qian, *Nature Photonics*, 2015, **9**, 259–266.
7. T.T. Xuan , J.Q. Liu , R.J. Xie , H.L. Li, Zhuo Sun, *Chem. Mater.*, 2015, **27**, 1187–1193.
8. Q. Jin, Y. Hu, Y. Sun, Y.Li, J. Huo, X. Zhao, *RSC Adv*., 2015,**5**, 41555–41562.
9. M. P. Hendricks, M. P. Campos, G.T. Cleveland, I. J.L. Plante, J. S. Owen, *Science*, 2015, **348**, 1226-1230.
10. H.N. Abdelhamid, H.F. Wu, *RSC Advances*, 2015, **5** , 50494-50504
11. H. N. Abdelhamid, Applications of Nanomaterials and Organic Semiconductors for Bacteria & Biomolecules analysis/biosensing using Laser Analytical Spectroscopy, M.Sc. thesis, National Sun-Yat Sen University, ROC, July 2013.
12. K. Shrivas, H.F. Wu. *J. Mass Spectrom*. 2010, **45,** 1452.
13. X. Dong, J. Cheng, J. Li, Y. Wang. *Anal. Chem*. 2010, **82,** 6208–6214.
14. C.K. Chiang, W.T. Chen, H.T. Chang. *Chem. Soc. Rev*. 2011, **40,** 1269-81.
15. P.A. Kuzema. *J. Anal. Chem*.2011, **66,** 1227-1242.
16. R. Pilolli, F. Palmisan, N. Cioffi. *Anal. Bioanal. Chem.* 2012, **402,** 601-23.
17. H.F. Wu, J. Gopal, H.N. Abdelhamid, N. Hasan. *Proteomics*. 2012, **12,** 2949–2961.
18. L. Messori, F. Scaletti, L.Massai, M. Agostina Cinellu, I. R. Krauss, G. di Martino, A. Vergara, L. Paduano, A. Merlino, *Metallomics*, 2014, **6**, 233-236.
19. Y.R. Zheng , K. Suntharalingam , T. C. Johnstone , H. Yoo , W. Lin , J. G. Brooks , S. J. Lippard , *J. Am. Chem. Soc.*, 2014, **136**, 8790–8798.
20. X.F. Zhao, Y. Ouyang, Y.Z. Liu, Q.J. Su, H. Tian, C.Z. Xie and J.Y. Xu, *New J. Chem*., 2014, **38**, 955-965.
21. M. Jarosz, M. Matczuk, K. Pawlak, A.R. Timerbaev, *Anal.Chim. Acta*, 2014, **851**, 72–77.

22. J. R.Perkins, M. Sanak, G. Canto, M. Blanca, J. A. Cornejo-Garcia, *Trends in Pharmacological Sciences*, 2015, **36**, 172-183.

23. X. Sun, C.N. Tsang, H. Sun, *Metallomics*. 2009, **1,** 25–31.

24. H. N. Abdelhamid, H.F. Wu, *RSC Adv*., 2014, **4**, 53768-53776.

25. C.H. Leung, S. Lin, H.J. Zhong, D.L. Ma, *Chem. Sci*., 2015, **6**, 871-884.

26. F. Lanucara, S. W. Holman, C. J. Gray, C. E. Eyers, *Nature Chemistry* 2014, **6**, 281-294; (b) C.G. Vogiatzis, G.A. Zachariadis, *Anal. Chim. Acta*, 2014, **819**, 1–14

27. H. N. Abdelhamid, H.F. Wu, *Mass Spectrom. Lett*. 2015, **6**, 43–47.

28. M.F. Wyatt, *J. Mass. Spectrom*, 2011, **46,** 712–719.

29. Y. Kea, S.K. Kailasa, H.F. Wu, Z.Y. Chen. *Talanta*. 2010, **83,** 178–184.

30. S. Huang, F. Zhu, Q. Xiao, Q. Zhou, W. Su, H. Qiu, B.Hu, J. Sheng and C. Huang, *RSC Adv*., 2014, **4**, 36286-36300.

31. H. Venkataraman, M.W.den Braver, N.P.Vermeulen, J.N. Commandeur. *Chem Res Toxicol*. 2014; **27**, 2071-2081.

32. H.N. Abdelhamid, H.F. Wu, *J. Am. Soc. Mass Spectrom*. 2014, **25**, 861-868.

33. W.W. Yu, X. Peng. *Chem., Int. Ed.* 2002, **41,** 2368-2371.

34. H.N. Abdelhamid, H.F. Wu. *Talanta* 2013, **115,** 442–450.

35. M. Edriss, N. Razzahi, B. Madjidi. *Turk. J. Chem*. 2008, **32,** 505 – 519.

36. H.N. Abdelhamid, H.F. Wu. *J. Mater. Chem. B*, 2013, **1**, 3950-3961.

37. J. Gopal, H.N. Abdelhamid, P.Y. Hua, H.F. Wu. *J. Mater. Chem. B* 2013, **1,** 2463-2475

38. H.N. Abdelhamid, H.F. Wu. *Colloids and Surfaces B: Biointerfaces*. 2013, **115,** 51–60.

39. H.N. Abdelhamid, H.F. Wu, *Trends. Anal. Chem.*. 2015, **65**, 30-46.

40. J. Joo, Y.W. Kim, Z. Wu, J.H. Shin, B. Lee, J. C. Shon, E.Y. Lee, N. M. Phuc, K.H. Liu, *Biopharmaceutics & Drug Disposition*, 2015, **36**, 258–264.

41. M.V. Gomez-Gaviro, I. Gonzalez-Alvaro, C. Dominguez-Jimenez, J. Peschon, R.A. Black, F. Sanchez-Madrid, F. Diaz-Gonzalez, *J. Biol. Chem*. 2002, **277**, 38212–38221.

42. F. Dimiza, S. Fountoulaki, A. N. Papadopoulos, C. A. Kontogiorgis, V. Tangoulis, C. P. Raptopoulou, V. Psycharis, A. Terzis, D. P. Kessissoglou and G. Psomas, *Dalton Trans*., 2011, **40**, 8555-5568.

43. Y. Koizumi, A. Sato, T. Yamada, M. Inada., *Clin Exp Pharmacol Physiol*. 1984, **11**, 291-299.

44. J. Feng, X. Du, H. Liu, X. Sui, C.Zhang, Y. Tang, J. Zhang. *Dalton Trans*. 2014, **43**, 10930-10939

45. F. Dimiza, A. N. Papadopoulos, V. Tangoulis, V. Psycharis, C. P. Raptopoulou, D. P. Kessissoglou and G. Psomas, *Dalton Trans*., 2010, **39**, 4517-4528.

46. X. Totta, A.A. Papadopoulou, A.G. Hatzidimitrou, A. Papadopoulos, G. Psomas Synthesis, *J. Inorg. Biochem*., 2015, **145**, 79-93.

47. M. A. Carvalho, E. G.R. Arruda, D. M. Profirio, A. F. Gomes, F. C. Gozzo, A. L.B. Formiga, P. P. Corbi, *J. Molecular. Structure*, 2015, **1100**, 2015.

Table 1: pH and conductivity of ponstel drug and metallodrug at 25 ± 2 °C

Compound/metallodrug	**pH**	**Conductivity (Scm^{-1})**
Ponstel	4.66	121.0
Fe(III)-Ponstel complex	2.90	217.8
Cu(II)-Ponstel complex	4.22	145.8

Table 2: Comparison between traditional MALDI and QELDI-MS

Technique	**Analyte**	**Volume (μL)**	**LOD (M)**
MALDI-MS	$[M+H]^+$	0.5	2×10^{-4}
	$[^{63}Cu(M-H)_2+H]^+$	0.5	Not detected
	$[^{56}Fe(M-H)_3+H]^+$	0.5	Not detected
QELDI-MS	$[M+H]^+$	0.5	1×10^{-4}
	$[^{63}Cu(M-H)_2+H]^+$	0.5	5×10^{-4}
	$[^{56}Fe(M-H)_3+H]^+$	0.5	5×10^{-4}